Met Office

Evaluating atmospheric absorption models using ISMAR

Stuart Fox, Vinia Mattioli, Emma Turner, Alan Vance, Domenico Cimini, Donatello Gallucci

ARTS workshop, Kristineberg, May 2024

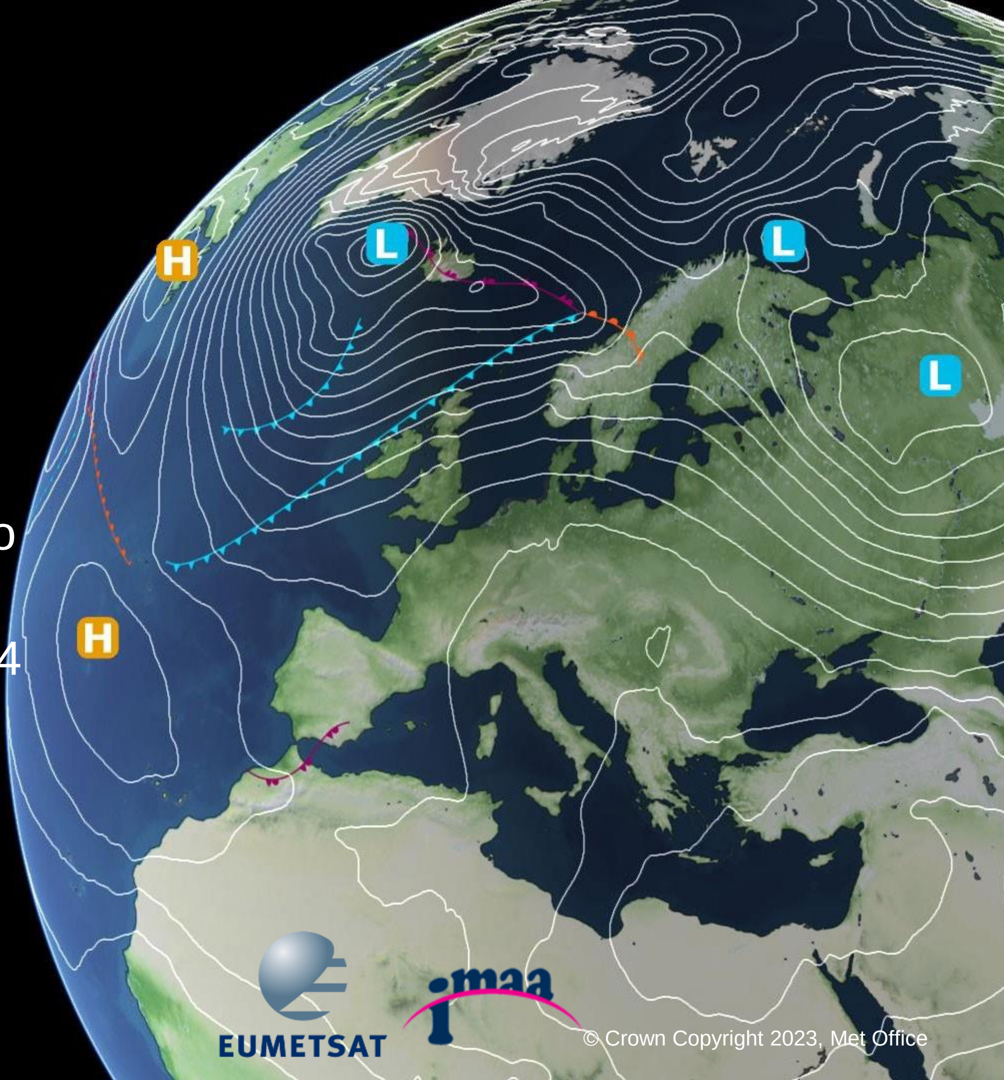

Met Office

Passive submillimetre radiometry: A new method for ice cloud remote sensing

EPS-SG Satellite B1 due to launch Dec 2025, carries Ice Cloud Imager (ICI)

Image: EUMETSAT

IR only sensitive to cloud top for optically thick clouds

Lidar/Radar have very limited spatial coverage

ICI retrieval products:

- Ice water path (column ice mass)
- Mean particle diameter
- Mass-mean cloud height

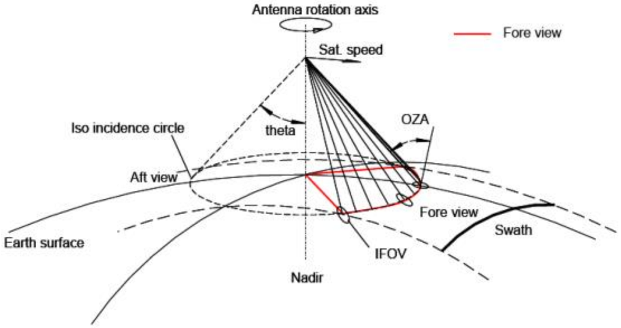

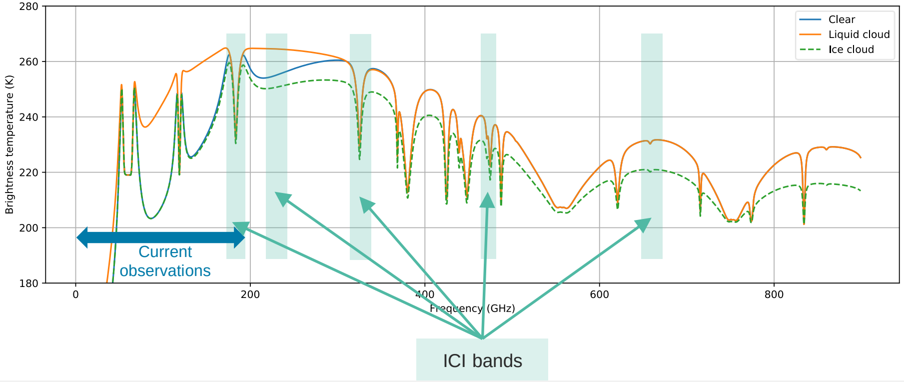

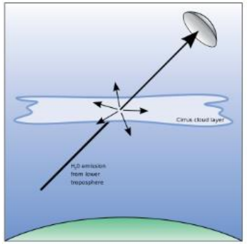

Retrieval Challenges

- Non-linear relationship between ice mass and brightness temperatures
- Non-Gaussian statistics
- Multiple-scattering (polarised) radiative transfer model required
- Complex and variable ice crystal shapes (and scattering properties)
- Uncertainties in ice size distribution

EUMSTSAT study overview

- EUMETSAT-funded study
- Recommend clear-sky absorption model for use with ICI
- Accurate clear-sky absorption needed for:
  - Cal/val of radiometric accuracy
  - Calculating cloud-induced BT depression
  - Detection of thin clouds
  - Extracting humidity information

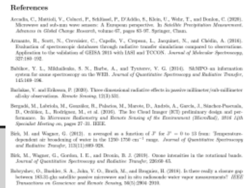

Literature Review
- Identify current knowledge and uncertainties
- Recommend absorption models to evaluate

Lead: Met Office

Airborne dataset
- Develop dataset using new and existing observations from FAAM aircraft
- Use dataset to evaluate recommended models

Lead: Met Office

Ground-based observations
- Obtain new high-spectral –resolution observations from APEX observatory
- Use observations to evaluate absorption models

Lead: Estellus, CSIC

Characterize Uncertainty
- Identify key uncertainties and correlations in spectroscopic parameters
- Propagate uncertainties to determine impact on simulated brightness temperatures

Lead: CNR

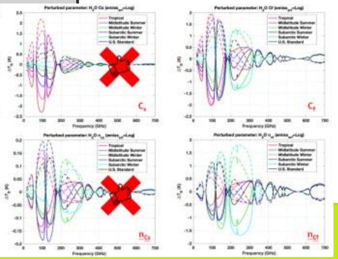

https://nwp-saf.eumetsat.int/site/download/members_docs/cdop-3_reference_documents/NWPSAF_report_submm_litrev.pdf
https://doi.org/10.5194/egusphere-2023-3160
https://doi.org/10.1051/0004-6361/202243409

Met Office

In AMSUTRAN, used for RTTOV-13 ICI coefficients

Feature	AER	PWR19
Updates	Active on-going work to refine parameters	Regularly updated with new parameters
Spectral range	Microwave to ultra-violet	Microwave to sub-millimetre
Sources	Field campaigns constrain key parameters	Majority from various laboratory studies
Lineshape	Voigt using the Humlíček (1982) approximation	VVW with optional speed-dependent shape ... lines
H_2O lines	Hundreds included, nine below 10... constrained: 22.23, 183.31, 325.15, ... 556.93, 620.70, 752.03, 916.17, 987.9...	...325.15, ...474.68, ...
Pressure shifts	Air-broadened	Air and self-broadened
H_2O continuum	MT-CKD model at 300 GHz increments updated regularly based on new campaigns	Turner et al. (2009) continuum parameters adjusted slightly for new line parameters
O_2 lines	Tretyakov et al. (2005) parameters	Parameters from various recent studies
Line mixing	First order from Tretyakov et al. (2005)	Second order from Makarov et al. (2018)
Uncertainties	Few specific estimates and HITRAN ranges	Most can be sourced from original study

Most recent version at time of review. Airborne analysis used updated 2022 version.

Literature review

- Review of literature for spectroscopy relevant to ICI
- Compares different sources of data (e.g. HITRAN, AER, studies of individual lines/parameters)
- Compares of spectroscopic parameters for key absorption lines, including uncertainties where available
- Published as NWP-SAF report

Parameter	S	γ_{air}	n_{air}	γ_{self}	n_{self}	δ_{air}	δ_{self}
units	$\frac{cm^{-1}}{molecules \times cm^2}$	$\frac{cm^{-1}}{atm}$	-	$\frac{cm^{-1}}{atm}$	-	$\frac{cm^{-1}}{atm}$	$\frac{cm^{-1}}{atm}$
22.235 GHz							
AER 3.8	4.348e-25[a]	0.0917[b]	0.65[?]	0.385[c]	0.65[?]	-0.800e-3[?]	-
	0.5%	0.00275 (*3%*)[g]	-	*>20%*	-	0.989e-3 (*121.9%*)[d]	-
PWR19	4.454e-25[e]	0.0912[f]	0.76[g]	0.449[f]	1.2[h]	-1.115e-3[f]	27.51e-3[f]
	1%	0.00062 (*0.68%*)	-	0.00148 (*0.33%*)	0.5 (*41.67%*)	0.127e-3 (*11.40%*)	0.303e-3 (*1.10%*)
183.31 GHz							
AER 3.8	7.691e-23[a]	0.1025[b]	0.71[i]	0.519[c]	0.71[i]	-2.700e-3[g*]	-
	0.5%	0.00238 (*3%*)[g]	-	*≥10% <20%*	-	0.989e-3 (*36.79%*)[j]	-
PWR19	7.736e-23[e]	0.0995[h]	0.77[g]	0.499[h]	0.78[h]	-2.433e-3[h]	5.830e-3[h]
	1%	0.0005 (*0.51%*)	-	0.0127 (*2.5%*)	0.08 (*10.26%*)	0.254e-3 (*10.42%*)	0.761e-3 (*13.04%*)
325.15 GHz							
AER 3.8	9.012e-23[a]	0.0944[k]	0.73[?]	0.507[c]	0.73[?]	-2.000e-3[?]	-
	0.5%	*≥5% <10%*	*≥5% <10%*	*≥10% <20%*	*≥5% <10%*	*≥0.001 < 0.01*	-
PWR19	9.077e-23[e]	0.0962[l]	0.64[m]	0.471[l]	0.74[n]	-0.439e-3[l]	44.7e-3[l]
	1%	0.00071 (*0.74%*)	0.09 (*14.06%*)	0.00071 (*0.16%*)	-	0.167e-3 (*38.10%*)	0.020e-3 (*0.45%*)
448.00 GHz							
AER 3.8	8.625e-22[s]	0.0889[j]	0.65[o]	0.467[p]	0.65[n]	-3.100e-3[?]	-
	≥5% <10%	*≥5% <10%*	*≥2% <5%*	*≥2% <5%*	*≥2% <5%*	*≥0.001 < 0.01*	-
PWR19	8.633e-22[e]	0.0883[q*]	0.70[r]	0.440[q]	0.67[n]	-3.291e-3[q]	-20.786e-3[q]
	≥1% <2%	0.0333 (*0.96%*)		0.00076 (*0.17%*)	-	0.43e-3 (*11.04%*)	0.89e-3 (*4.27%*)
556.94 GHz							
AER 3.8	5.207e-20[s]	0.1103[b]	0.75[r]	0.487[p]	0.75[r]	6.800e-3[?]	-
	≥5% <10%	*4.1%*	*<1%*	*≥1% <2%*	*<1%*	*≥0.001 < 0.01*	-
PWR19	5.238e-20[e]	0.1053[s]	0.75[q]	0.481[s]	1.00[n]	6.326e-3[s]	-57.22e-3[s]
	≥1% <2%	0.00045 (*0.43%*)	*<1 %*	0.0051 (*1.06%*)	-	0.45e-3 (*7.17%*)	2.56e-3 (*4.47%*)
752.03 GHz							
AER 3.8	3.433e-20[t]	0.1072[b]	0.77[r]	0.463[p]	0.77[r]	8.500e-3[?]	-
	≥5 % <10 %	*4.9 %*	*<1 %*	*≥1 % <2 %*	*<1 %*	*≥0.001 < 0.01*	-
PWR19	3.454e-20[e]	0.1052[u]	0.77[q]	0.459[u]	0.84[n]	5.48e-3[u]	-29.66e-3[u]
	≥1 % <2 %	0.0012 (*1.12%*)	*<1 %*	0.0038 (*0.83%*)	-	0.68e-3 (*12.5%*)	0.76e-3 (*2.56%*)

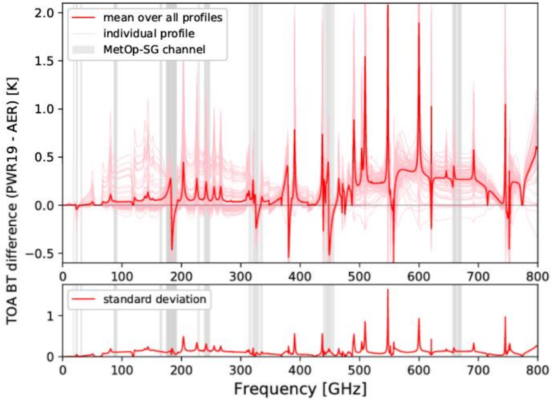

Figure 37: TOA brightness temperature differences between PWR19 and the AER model (AER v3.8 lines and MT-CKD 3.5 continuum), due to water vapour only. Simulations are made using the 83 diverse atmospheric profile with nadir viewing geometry and an emissivity of 1. The coverage of MetOp-SG channels are shaded grey.

- Recommends two (water vapour) spectroscopic configurations for further study
- These are self-consistent, but follow different philosophies
- Non-negligible differences between these two models for TOA brightness temperatures at ICI frequencies

“AER” (AMSUTRAN) implementation in ARTS

Line catalogs created in ARTS XML format:

- AER v3.8 “fast” H2O line catalog (338 lines)
- Custom O3 line catalog (based on JPL, 652 lines)
- Set `mirroring_option` to None and use `abs_lines_per_speciesManualMirroringSpecies`
- Use `ByLine` cutoff option, with `cutoff_value=750e9`

`MT-CKD v3.5` continuum (now available in ARTS)

`O2-TRE05`

`N2-SelfContMPM93`

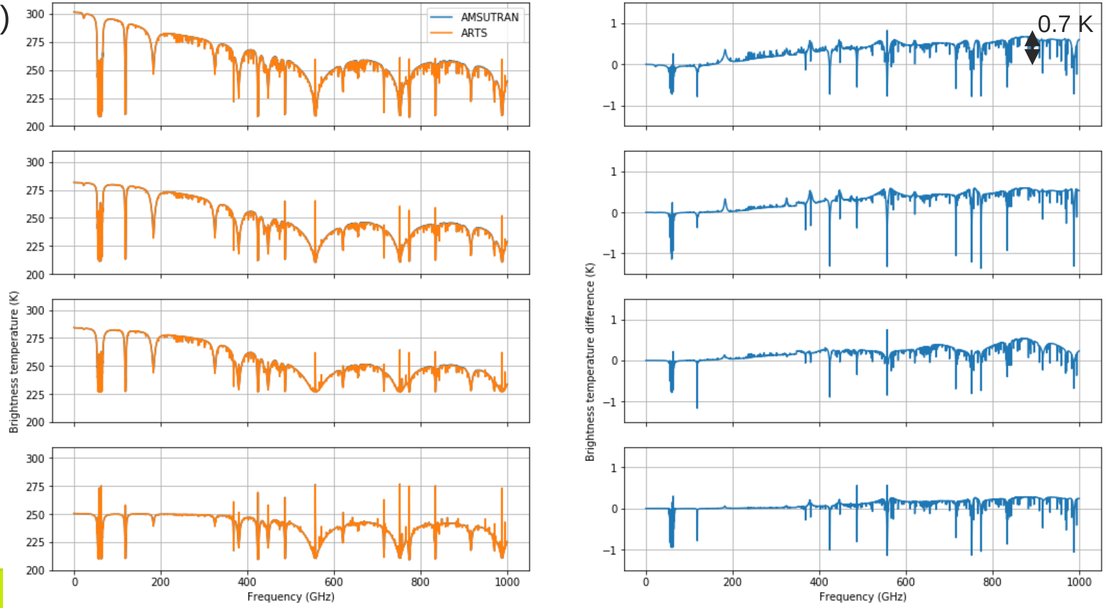

Comparison of absorption coefficients

- A couple of bugs in AMSUTRAN absorption implementation identified and fixed
- ARTS O2-TRE05 has "feature" related to isotopic abundance. Need to set O2 VMR to 0.2085 rather than 0.2095
- Temperature-dependence of pressure-induced line shift differs
- Difference in H2O TIPS values – mainly affects minor isotopologues.

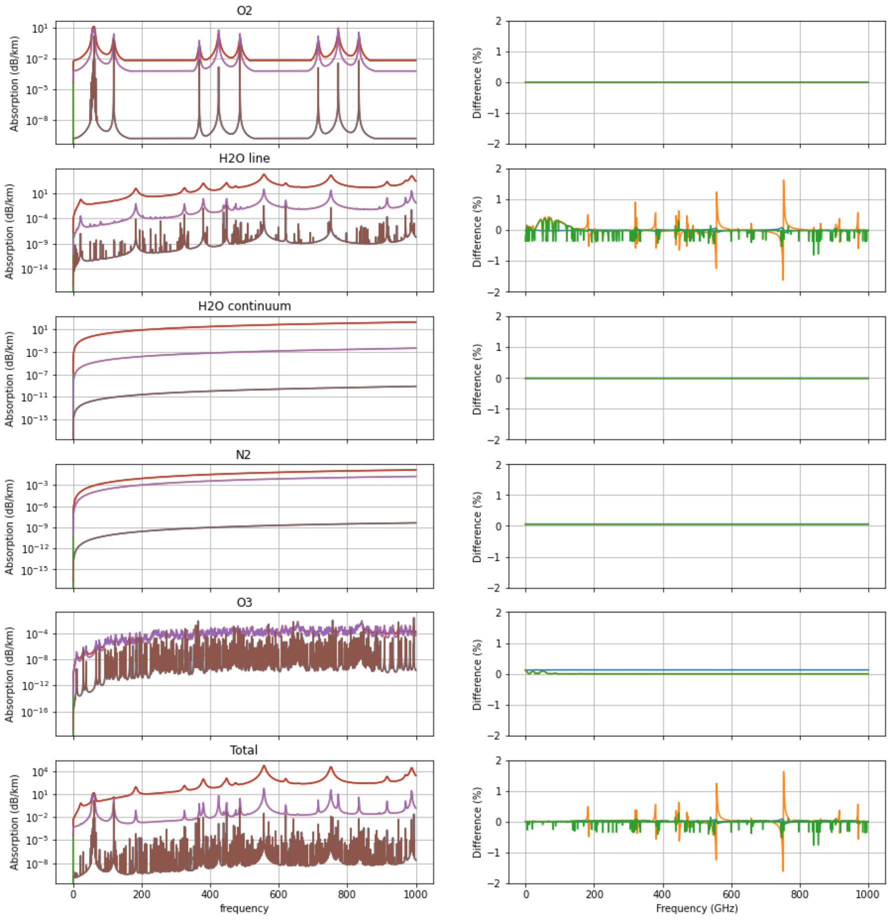

Met Office

Final BT comparison

- Remaining differences primarily due to implementation of RT calculation
- To get this level of agreement need high vertical resolution in ARTS calculation `ppath_lmax=100`

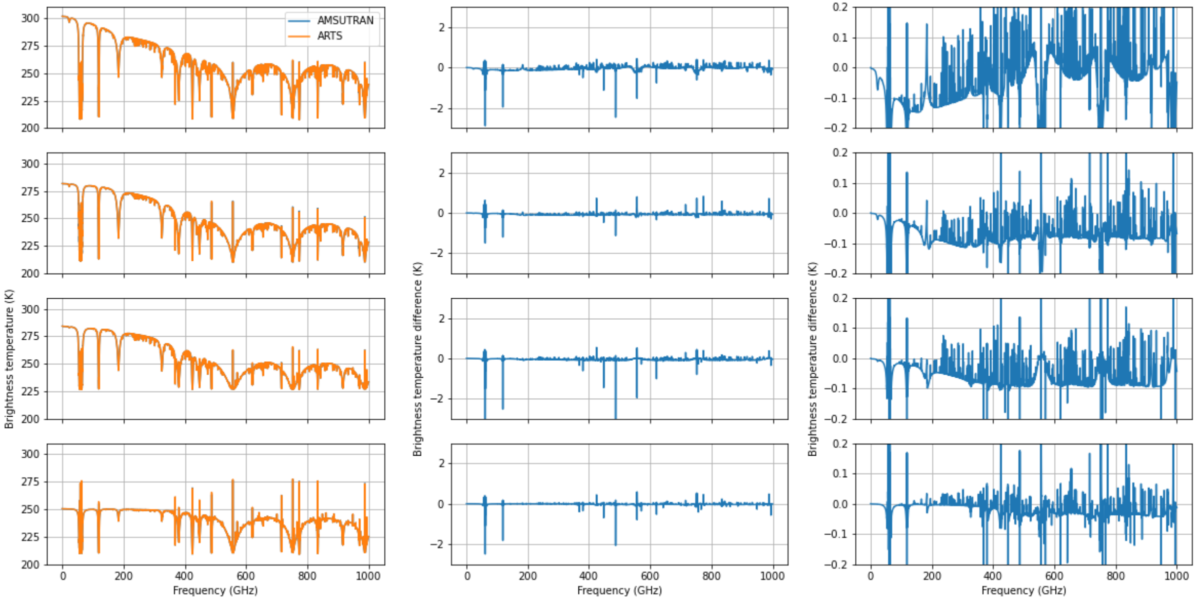

“Rosenkranz” models

- New “PWR” complete absorption models now available in ARTS – PWR2021 and PWR2022 for H_2O and O_2, PWR2021 for N_2
- Comparison with CNR implementation within ~0.05% for absorption coefficient
- Brightness temperature mostly within 0.4K – difference due to RT implementation and reduces with increased vertical resolution

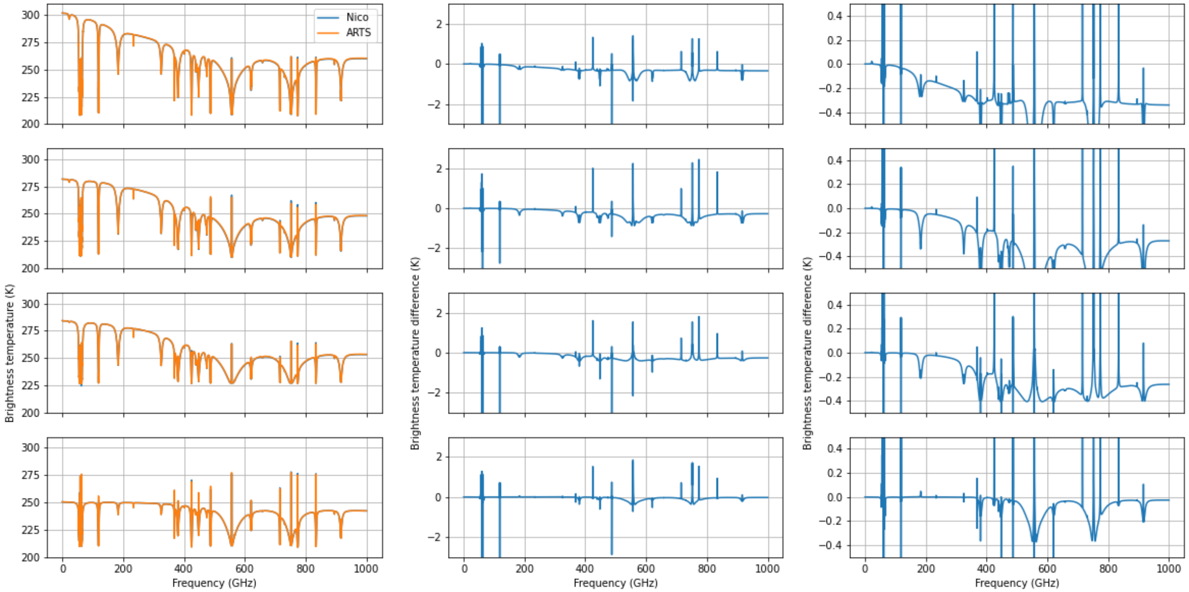

Met Office

Airborne dataset

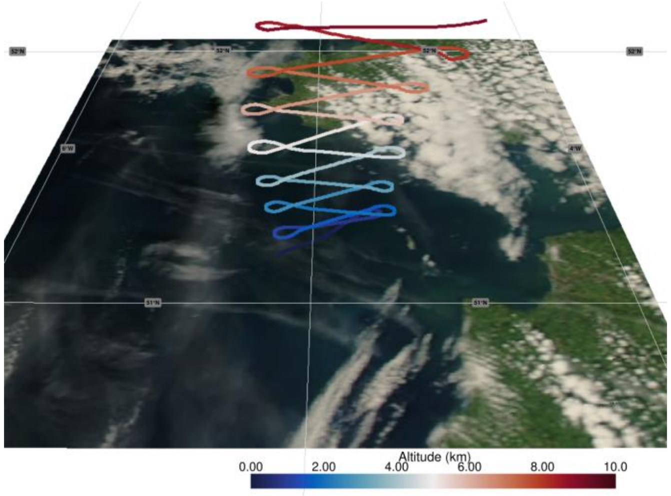

Data from 13 FAAM flights between 2015 and 2021, mostly around the UK

ISMAR/MARSS channel	MWI channel
89 GHz (mixed)	89 GHz (V and H)
118±1.1 GHz (V)	118±1.2 GHz (V)
118±1.5 GHz (V)	118±1.4 GHz (V)
118±2.1 GHz (V)	118±2.1 GHz (V)
118±3 GHz (V)	118±3.2 GHz (V)
118±5 GHz (V)	
157 GHz (H)	165.6 GHz (V)

ISMAR/MARSS channel	ICI channel
183±7 GHz (H)	183±7 GHz (V)
183±3 GHz (H)	183±3.4 GHz (V)
183±1 GHz (H)	183±2 GHz (V)
243 GHz (V and H)	243 GHz (V and H)
325±9.5 GHz (V)	325±9.5 GHz (V)
325±3.5 GHz (V)	325±3.5 GHz (V)
325±1.5 GHz (V)	325±1.5 GHz (V)
448±7.2 GHz (V)	448±7.2 GHz (V)
448±3.0 GHz (V)	448±3.0 GHz (V)
448±1.4 GHz (V)	448±1.4 GHz (V)
664 GHz (V and H)	664 GHz (V and H)
874 GHz (V and H)	

Dataset overview

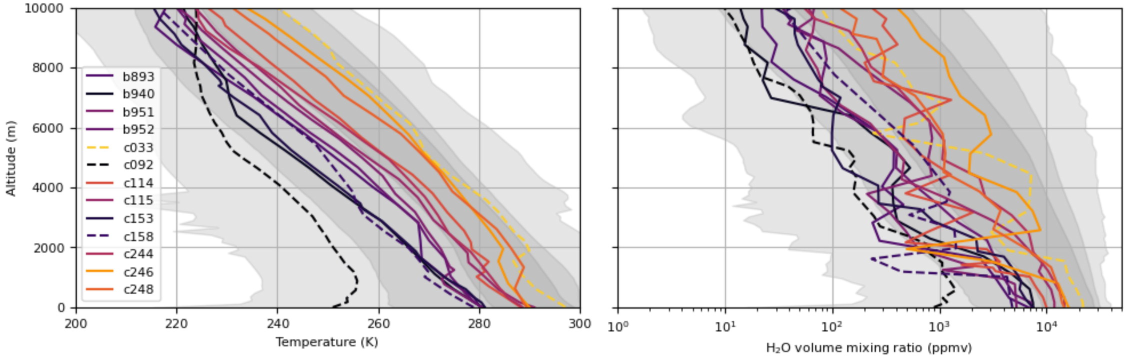

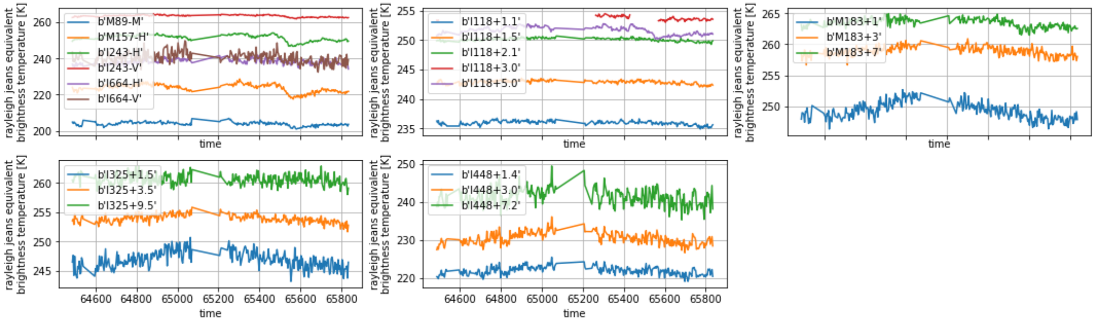

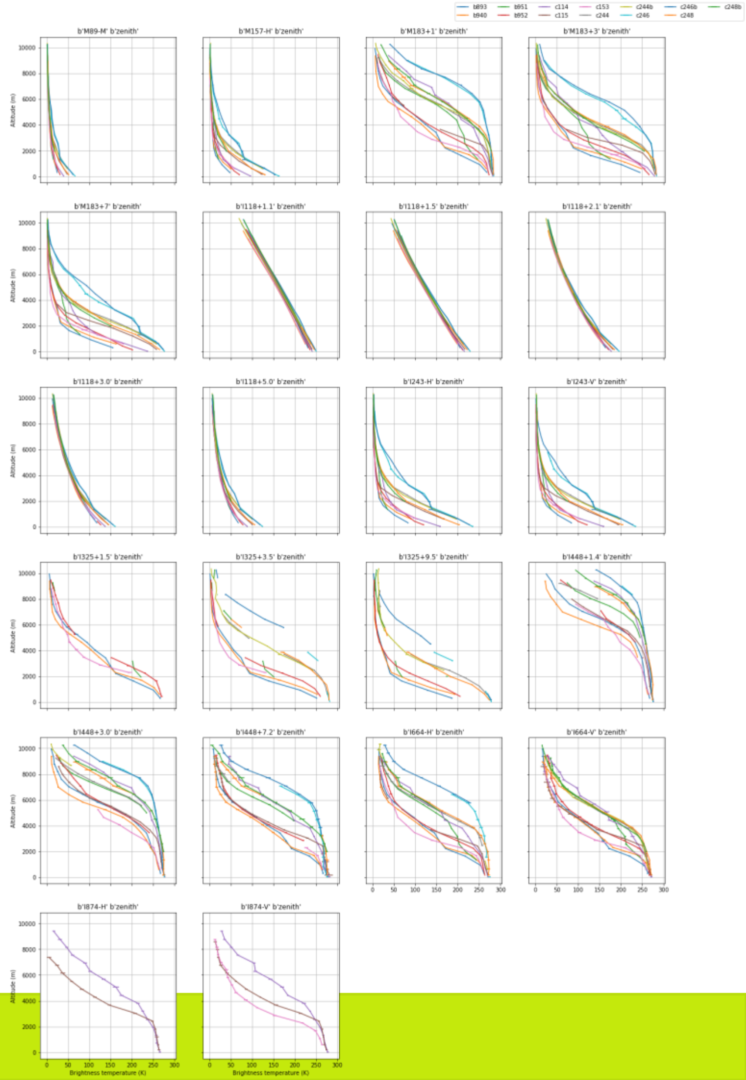

Met Office

Radiative closure

Inputs

- Best guess profiles + variability
- Recommended absorption model
- Channel characteristics

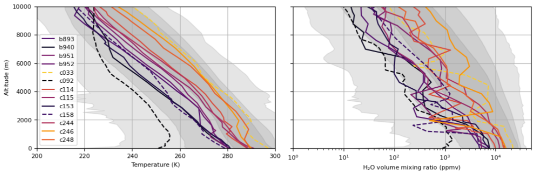

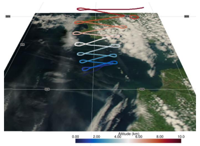

Simulation

- ARTS radiative transfer model

ARTS

Output

- Simulated brightness temperatures
- Compare simulations and observations

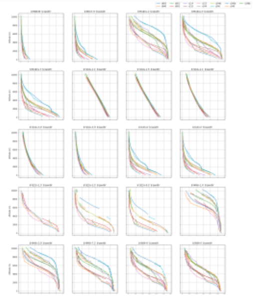

Closure results – AER/AMSUTRAN

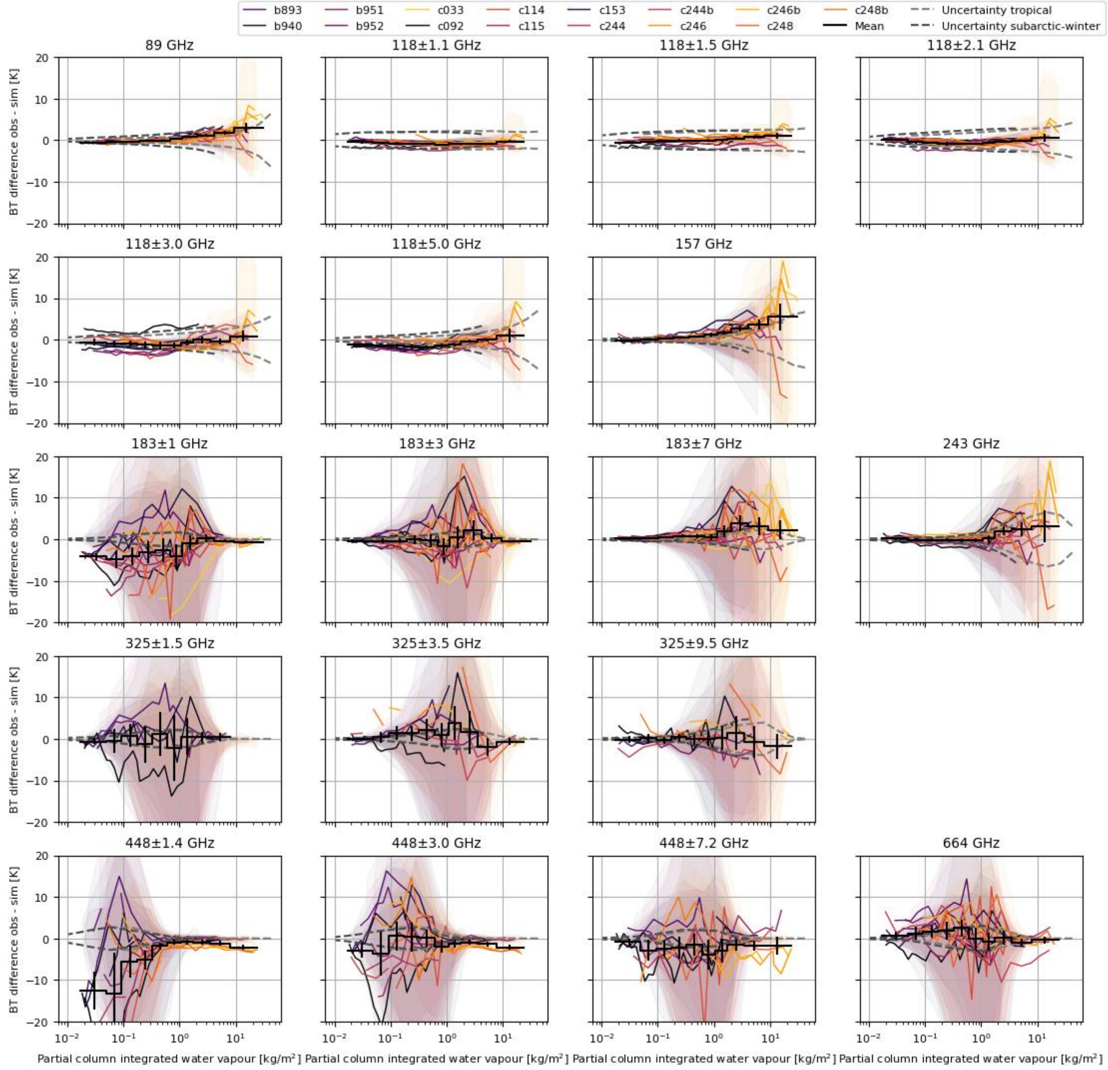

Atmospheric profile retrieval

Inputs
- Best guess profiles + errors
- Observed brightness temperatures

Retrieval
- ARTS radiative transfer model + OEM retrieval

Output
- Adjusted atmospheric profiles

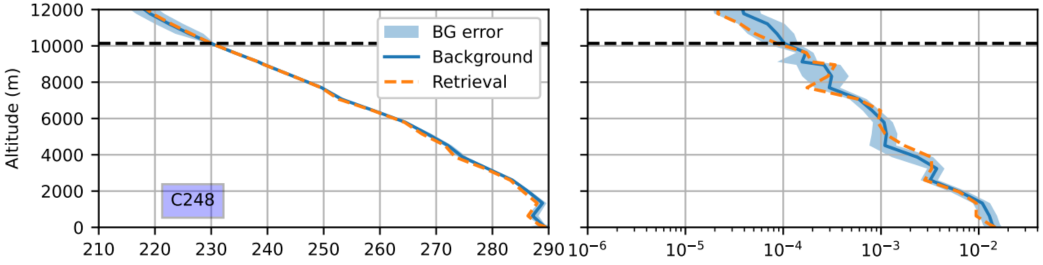

Retrieval results – AER/AMSUTRAN

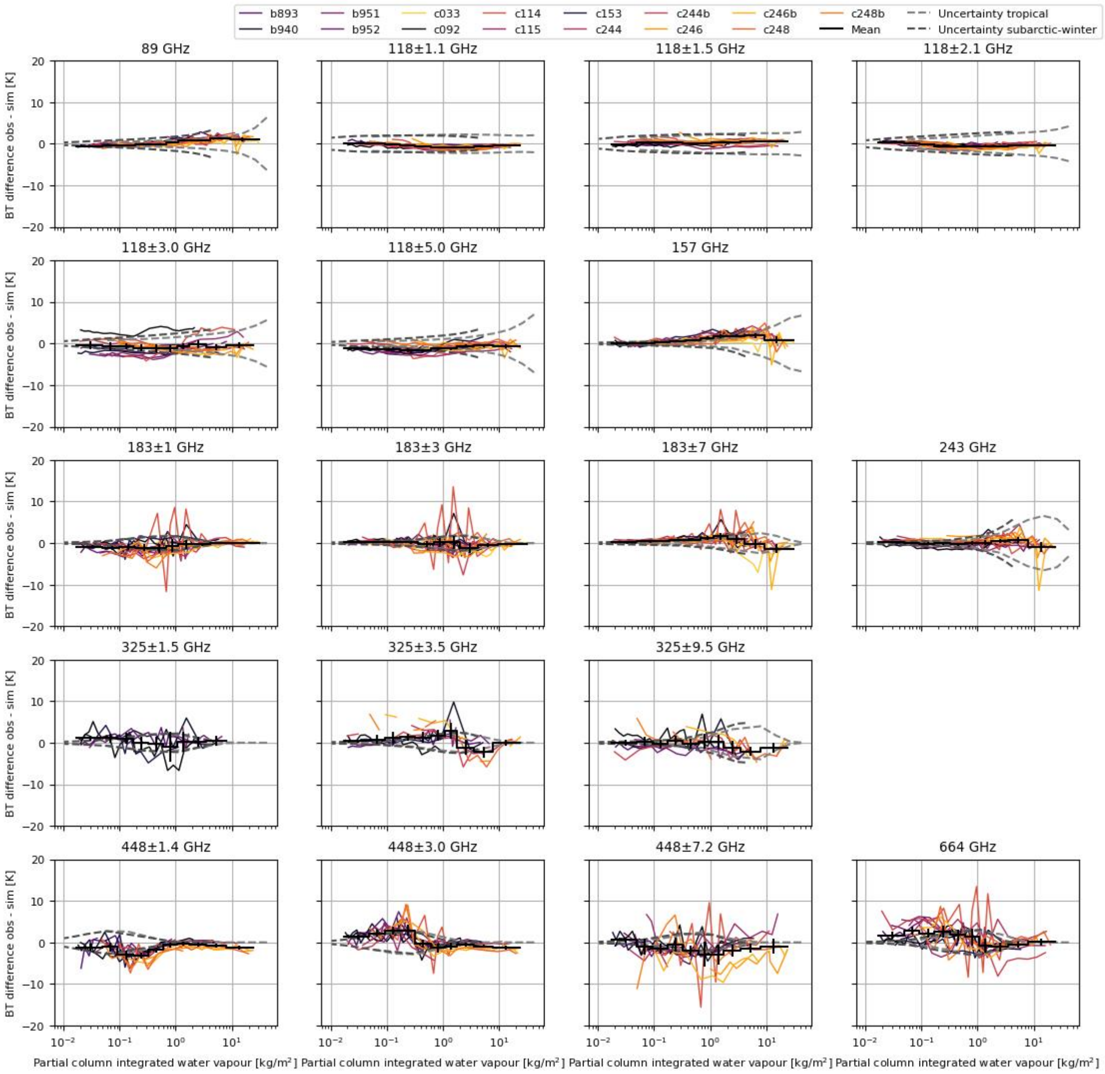

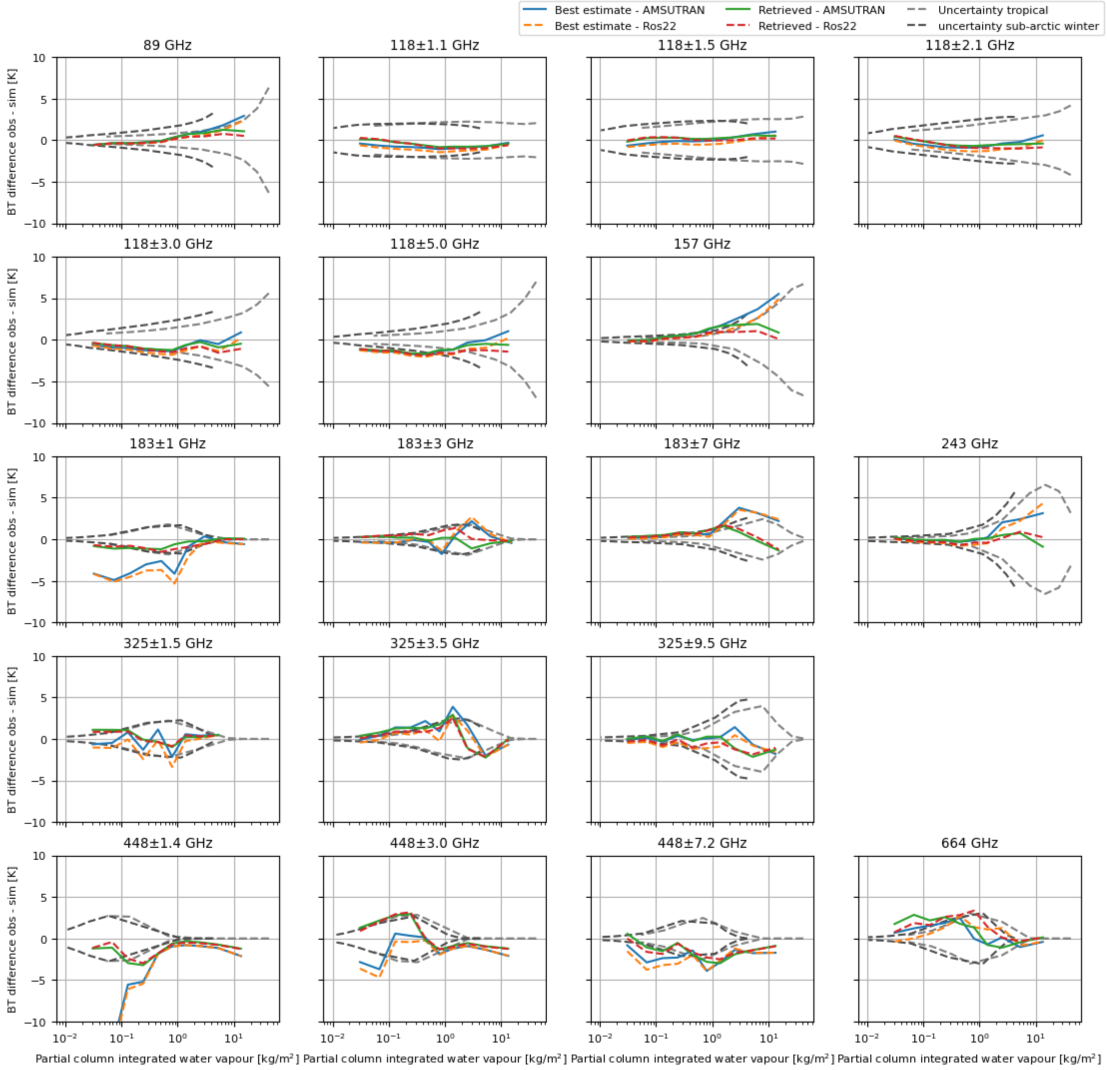

Comparison of AER & PWR

	Best guess (K)		Retrieved (K)	
Channel	AMSUTRAN	Ros22	AMSUTRAN	Ros22
89 GHz	0.85	0.67	0.58	0.42
118±1.1 GHz	0.75	1.07	0.50	0.63
118±1.5 GHz	0.37	0.47	0.31	0.15
118±2.1 GHz	0.57	0.86	0.46	0.69
118±3.0 GHz	0.86	1.15	0.75	1.02
118±5.0 GHz	1.14	1.40	1.11	1.45
157 GHz	1.67	1.18	0.94	0.50
183±1 GHz	2.50	2.98	0.66	0.76
183±3 GHz	0.67	0.73	0.33	0.51
183±7 GHz	1.40	1.27	0.80	0.80
243 GHz	0.88	1.09	0.30	0.38
325±1.5 GHz	0.88	0.98	0.62	0.58
325±3.5 GHz	1.45	0.98	1.30	1.03
325±9.5 GHz	0.53	0.82	0.64	0.74
448±1.4 GHz	4.41	4.66	1.36	1.24
448±3.0 GHz	1.50	1.68	1.43	1.42
448±7.2 GHz	2.13	2.47	1.56	1.46
664 GHz	1.01	1.00	1.49	1.50
Mean	1.31	1.41	0.84	0.85
Mean (>183 GHz)	1.58	1.70	0.95	0.95

Downward-looking closure

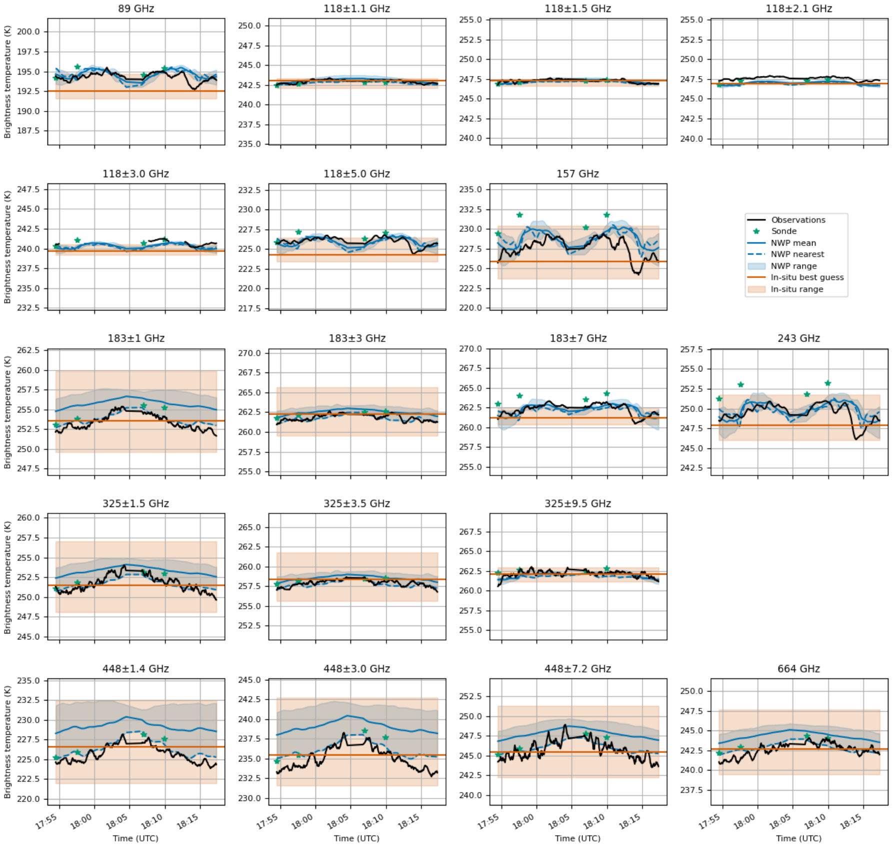

- Downward-looking views from high altitude compared to simulations
- Near-nadir views
- Simulations performed using atmospheric profiles and surface properties from:
  - Short-range high-resolution NWP model
  - Dropsondes
  - Aircraft in-situ measurements before/after high-altitude runs
- Only performed simulations for cloud-free scenes over the sea
  - TESSEM-2 surface emissivity model used

Downward-looking closure results

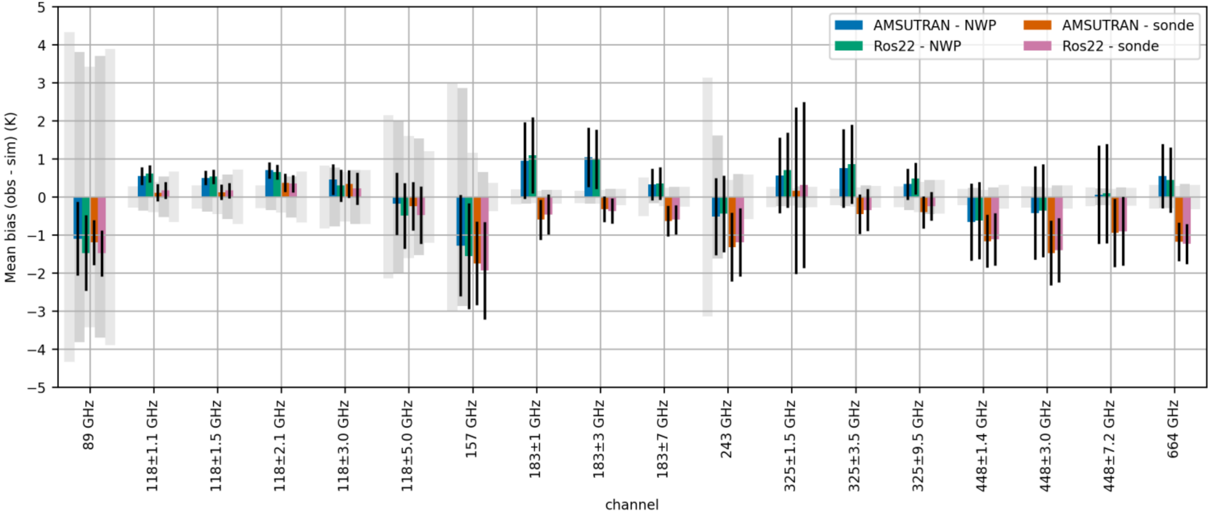

- Many channels show mean differences < 1K
- Some differences between sondes and NWP model (particularly for water vapour channels)
- Window-channel biases likely surface-related
- ICI radiometric accuracy ~1.5K

Met Office

Conclusions and recommendations

- A dataset of observations from FAAM aircraft was developed and used to evaluate AER and PWR absorption models, implemented within ARTS
- For individual flights, atmospheric profile uncertainty is the largest contributor to observation-model differences. This can be mitigated by averaging multiple flights or performing profile retrievals.
- Both AER and PWR spectroscopic models compare well with zenith and nadir observations
  - Mean differences mostly within 2K for zenith profiles
  - Mean differences mostly within 1K for nadir profiles
- Zenith observations mostly agree within spectroscopic uncertainty estimate. Nadir differences can be greater than spectroscopic uncertainty.
- Comparison with simulated brightness temperatures using radiosondes and NWP profiles will be a useful method to validate radiometric accuracy during ICI cal/val

EGUsphere - An evaluation of atmospheric absorption models at millimetre and sub-millimetre wavelengths using airborne observations (copernicus.org)

Extra slides

AER-Rosenkranz model difference

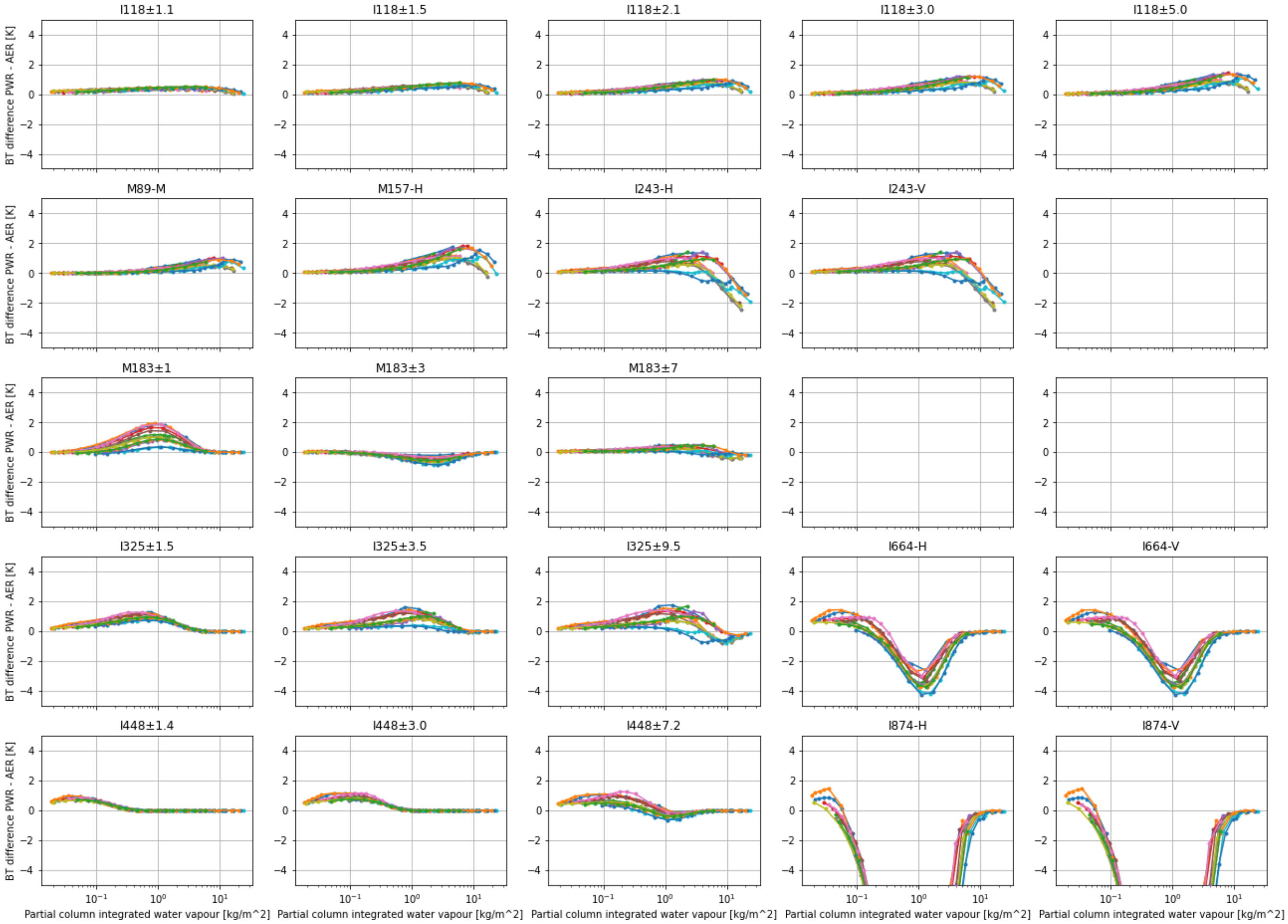

- Difference between modelled zenith brightness temperature for all profiles in dataset mostly <2K
- Exceptions are at 664 and 874GHz where contribution of lines > 1THz not present in Rosenkranz model is significant